A. MP2 - Inclusion of counterpoise in the optimisation step

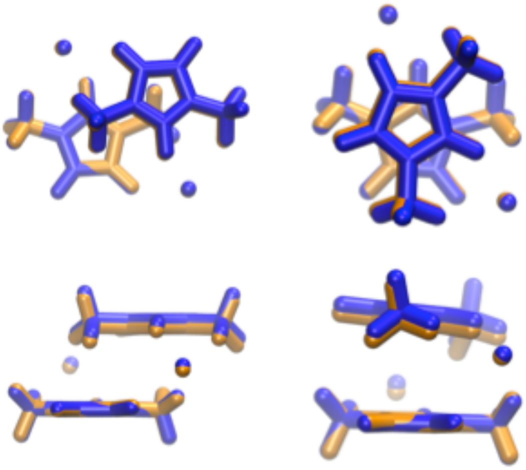

Figure S1. Top and side views of the M_FS_SF_A and M_FS_SF_R IP-dimer structures computed at the MP2 level with (orange) and without (blue) counterpoise included in the optimisation.

The inclusion of the counterpoise correction during geometry optimisation has previously been suggested to provide more accurate π-π geometries for the benzene dimer.[1] This has been tested for the M_FS_SF_A and M_FS_SF_R IP-dimer conformers. Optimisations were carried out with and without counterpoise correction at the MP2/aug-cc-pVDZ level.

The resulting structures are shown overlayed in Figure S1. The inclusion of the counterpoise correction results in slightly less contracted structures. This variation is primarily a vertical displacement with a difference of ≈0.1 Å for both the M_FS_SF_A and M_FS_SF_R IP-dimers. Geometries obtained with the inclusion of the counterpoise correction correspond well with the structures obtained at the B3LYP-D3 level without counterpoise correction. Thus, due to the additional computational cost (≈3x longer) a complete study of the IL IP-dimer structures employing the counterpoise correction is unjustified at present.

B. Estimating dispersion energy contribution for the ion pairs

Table S1. Estimate dispersion energy contribution in kJ/mol for the [C_1C_1im]Cl IP structures. Computed as the difference between B3LYP-D3 and B3LYP binding energies. A negative value indicates B3LYP-D3 binding energy is larger.

	ΔE_{Disp} (kJ/mol)
Front	-8.17
Top	-15.27
Side	-7.76
Back	-7.83

An estimate of the dispersion energy contribution for an IP is obtained from the difference in energy between the B3LYP-D3 and B3LYP levels (Table S1). For the IP structures the in-plane (front, side and back) structures have dispersion energy of ≈7 kJ/mol, which is approximately half of the energy for the top structure.

C. Data for [C_1C_1im]Cl ion-pairs

Table S2. Relative zero-point energy corrections (ΔZPE) in kJ/mol. Values reported relative to the [C_1C_1im]Cl IP front structure.

	B3LYP	**ωB97X**	**B3LYP-D2**	**ωB97X-D**	**B3LYP-D3**	**MP2**
Front	0.00	0.00	0.00	0.00	0.00	0.00
Top	1.85	1.79	2.79	2.32	2.81	0.76
Side	0.29	0.12	0.14	0.48	0.24	0.17
Back	0.10	0.32	0.37	0.55	0.40	-0.86

Table S3. ZPE and BSSE corrections, in kJ/mol, for the [C_1C_1im]Cl IP front structure.

	ZPE (kJ/mol)	**BSSE (kJ/mol)**
B3LYP	366.35	0.48
ωB97X	372.43	0.43
B3LYP-D2	364.88	0.48
ωB97X-D	370.45	0.41
B3LYP-D3	366.33	0.48
MP2	373.19	16.54

Table S4. Relative BSSE (ΔBSSE) in kJ/mol. Values reported relative to the [C_1C_1im]Cl IP front structure.

	B3LYP	**ωB97X**	**B3LYP-D2**	**ωB97X-D**	**B3LYP-D3**	**MP2**
Front	0.00	0.00	0.00	0.00	0.00	0.00
Top	-0.02	-0.43	-0.01	0.00	-0.01	-1.31
Side	0.01	0.00	0.01	0.01	0.00	-0.08
Back	-0.12	-0.13	-0.13	-0.12	-0.01	-5.99

Table S5. Free energy (ΔG), Enthalpy (ΔH) and Entropy (TΔS), in kJ/mol, for the $[C_1C_1im]Cl$ IP front structure.

	ΔG	ΔH	TΔS
B3LYP	-358.82	-388.36	-29.53
***ω*B97X**	-367.25	-397.63	-30.38
B3LYP-D2	-366.36	-395.84	-29.48
***ω*B97X-D**	-364.57	-394.56	-29.99
B3LYP-D3	-367.11	-396.48	-29.37
MP2	-379.10	-410.68	-31.59

Table S6. Relative free energies (ΔΔG) in kJ/mol. Values reported are reported relative to the $[C_1C_1im]Cl$ IP front structure.

	B3LYP	*ω*B97X	B3LYP-D2	*ω*B97X-D	B3LYP-D3	MP2
Front	0.00	0.00	0.00	0.00	0.00	0.00
Top	5.90	3.04	1.79	5.81	1.65	-0.50
Side	32.25	32.77	30.29	34.18	31.24	30.19
Back	56.42	58.96	57.87	59.86	57.42	55.84

Table S7. Relative enthalpies (ΔΔH) in kJ/mol. Values reported are reported relative to the $[C_1C_1im]Cl$ IP front structure.

	B3LYP	*ω*B97X	B3LYP-D2	*ω*B97X-D	B3LYP-D3	MP2
Front	0.00	0.00	0.00	0.00	0.00	0.00
Top	4.76	1.52	-1.88	3.48	-2.00	-0.87
Side	34.23	35.93	34.28	36.11	34.64	30.90
Back	62.59	62.93	63.43	64.58	63.13	60.40

Table S8. Relative entropies (ΔTΔS) in kJ/mol. Values reported are reported relative to the $[C_1C_1im]Cl$ IP front structure.

	B3LYP	*ω*B97X	B3LYP-D2	*ω*B97X-D	B3LYP-D3	MP2
Front	0.00	0.00	0.00	0.00	0.00	0.00
Top	-1.14	-1.52	-3.67	-2.33	-3.64	-0.38
Side	1.19	3.16	3.99	1.93	3.41	0.71
Back	6.17	3.97	5.56	4.72	5.71	4.56

D. Process for constructing 'possible' starting IP-dimer structures

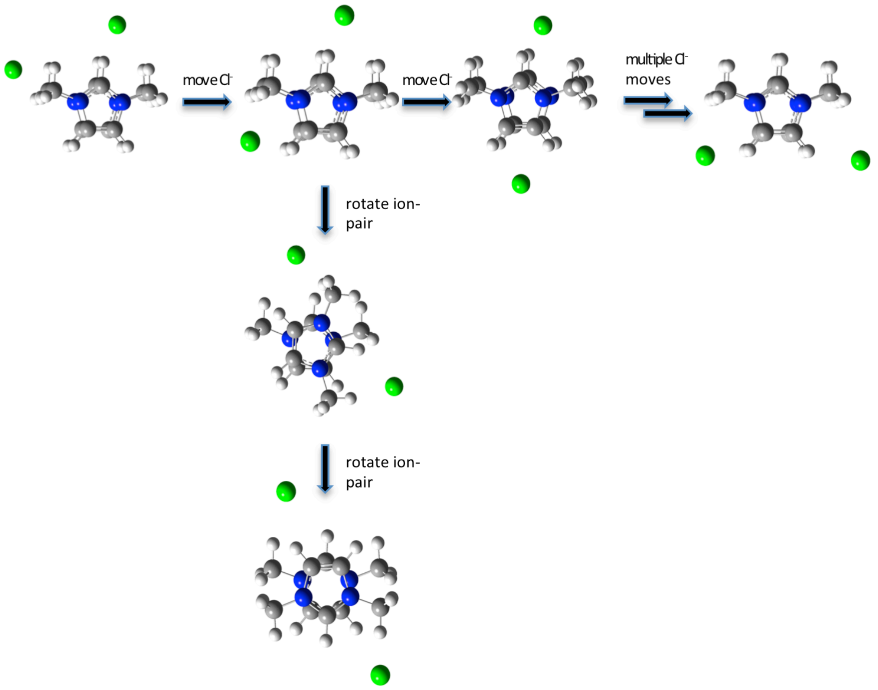

Figure S2. Representation of the process followed to generate the IP dimer starting structures.

The construction process is applied as follows, first two front IPs were arranged with $[C_1C_1im]^+$ rings parallel to each other in the xy-plane and the anions lay one above the other. The anion positions are then altered such that they lay within a plane equidistant between the $[C_1C_1im]^+$ rings, while remaining in out-of-plane front positions. This anion arrangement results in a clash of the anions. This is avoided by moving one of the anions (within the plane of the anions) to a shared meth position resulting in a structure with the rings parallel to each other and the anions in out-of-plane front and methyl positions. The position of the same anion was then systematically altered, leaving the out-of-plane front anion in position. This was achieved by moving it to alternate favourable in-plane cation-anion IP positions until all possible conformers had been generated. A further step which involved moving both anions so that they both occupied out-of-plane side positions on opposite sides of the $[C_1C_1im]^+$ rings was also carried out. Once all parallel *middle* conformers had been generated the top $[C_1C_1im]^+$ ring was rotated 90° in the z-axis to a 'rotated' ring orientation and the process of systematically placing the anions was repeated. The final stage involved a further 90° ring rotation around the z-axis to an antiparallel orientation and systematic placement of the anions. This general approach has been followed in the construction of *diagonal*, *alternate* and *outer* motifs.

E. Additional IP-dimer motifs

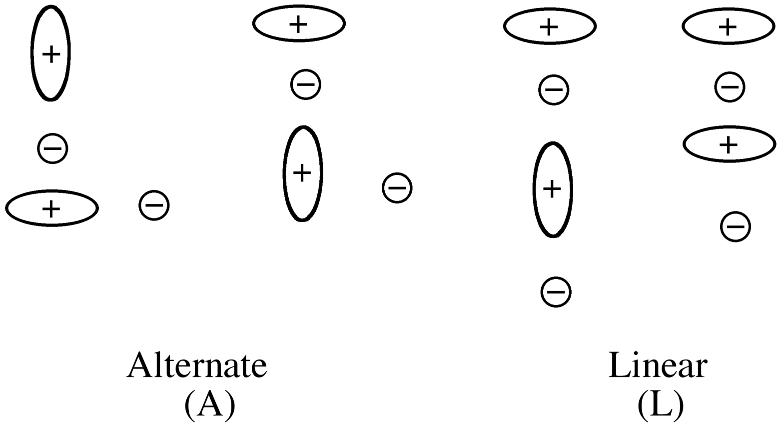

Figure S3. Additional alternate and linear IP dimer motifs considered in this work.

F. D_F1T_TF_A vs. D_F2T_TF_A and D_F1T_TF_T vs. D_F2T_TF_T

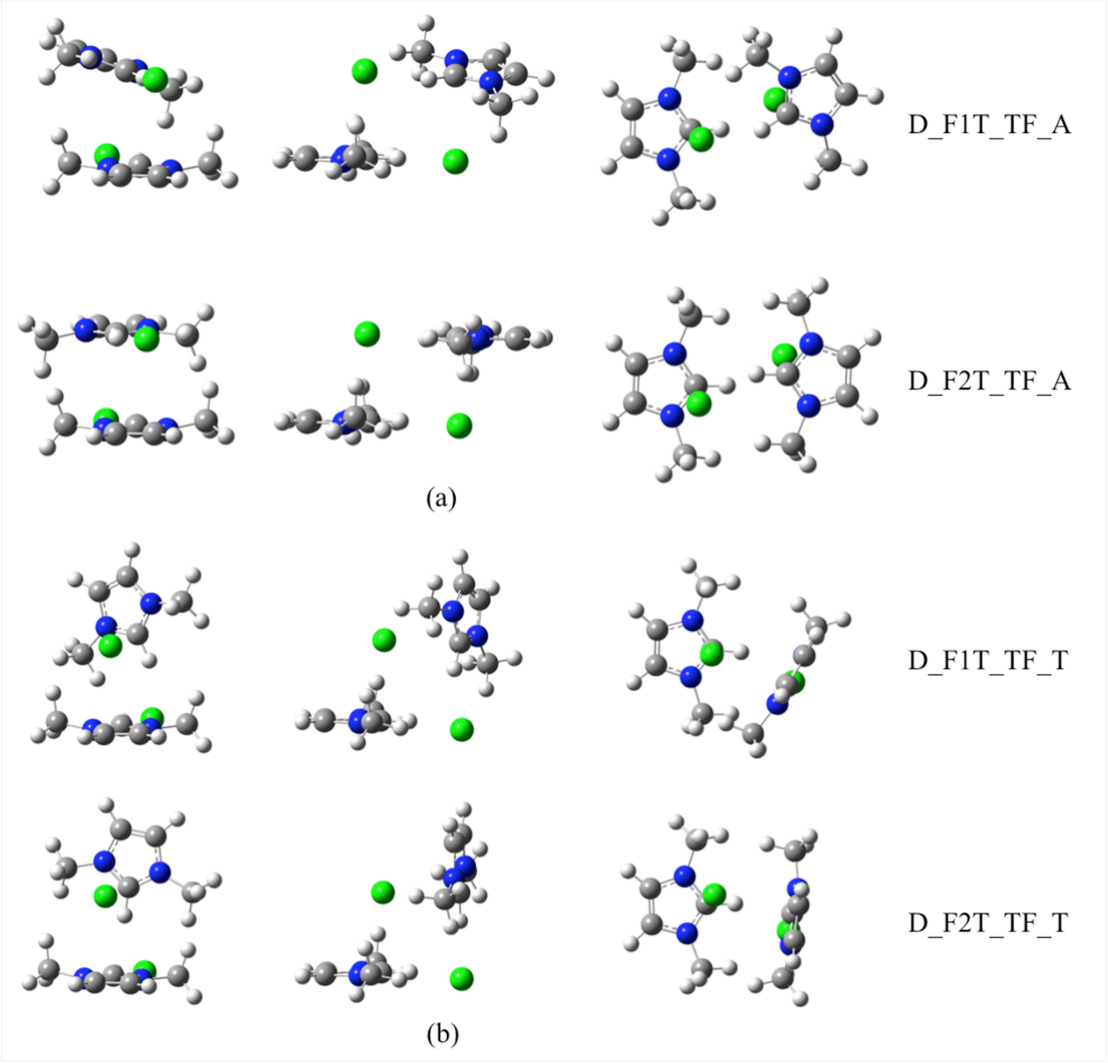

Figure S4. Front, side and top views of the (a) D_F1T_TF_A and D_F2T_TF_A and (b) D_F1T_TF_T and D_F2T_TF_T IP-dimer structures.

The D_FT_TF_A and D_FT_TF_A IP-dimer structures both have 2 distinct conformations. The conformers arise due to slightly different H-bonding motifs as shown in Figure S4a and S4b. Adding a 1 or 2 in the structures names allows us to differentiate between the conformers. The different H-bonding motifs give rise to a slight rotation of the upper imidazolium cation coupled with a concomitant twisting of the upper imidazolium cation from the parallel or T-shape. These structural features do not significantly alter the relative energies between the structures. The energy difference at the B3LYP-D3/aug-cc-pVTZ level between D_F1T_TF_A (2.32 kJ/mol) and D_F2T_TF_A (3.29 kJ/mol) conformers is ≈0.90 kJ/mol. The energy difference between and D_F1T_TF_T (3.68 kJ/mol) and D_F2T_TF_T (4.88 kJ/mol) is ≈1.20 kJ/mol. This indicates that these structures are very close and essentially appear as ripples on the $[C_1C_1im]Cl$ IP-dimer potential energy surface.

G. Binding energies and dispersion energy contributions for the IP-dimers

Table S9. Binding energies for the $[C_1C_1im]Cl$ IP-dimer structures (low and medium energies) in kJ/mol employing $\Delta E_B=E_{cluster}-2(\text{front IP})$

	B3LYP	B3LYP-D3
M_FS_SF_A	-83.60	-119.87
M_FS_SF_R	Not Stable	-119.45
M_FS_FS_R	-82.92	-118.22
D_F1T_TF_A	-86.12	-117.55
D_F2T_TF_A	-83.94	-116.58
D_F1T_TF_T	-84.88	-116.19
D_F2T_TF_T	-82.39	-114.99
M_FS_SF_P	-78.09	-112.38
M_SS_SS_A	-67.68	-93.28
D_TM_BF_T	-61.29	-86.97
D_TB_BT_A	Not Stable	-84.29
M_FB_BF_A	Not Stable	-82.46
D_TBt_BB_P	Not Stable	-71.05

IP-dimer binding energies may be be calculated using either constituent ions ($\Delta E_{B\text{-}ions}=E_{cluster}-2\times(E_{cation}+E_{anion})$) or IPs ($\Delta E_{B\text{-}ion\text{-}pair}=E_{cluster}-2\times(IP)$). The former approach was used in this work. This approach eliminates the need to choose which IP energies to use in the calculation, as the lowest energy IP may not always be the correct choice for IP-dimer structures that are not always a simple combination of specific IP conformers. $\Delta E_{B\text{-}ion\text{-}pair}$ for the M_FS_SF_A structure is -119.87 kJ/mol, whereas

$\Delta E_{B\text{-ions}}$ is -909.89 kJ/mol.

This discrepancy in binding energies is explained by remembering -909.89 kJ/mol is the energy of formation of an IP-dimer from two IPs. Combining the energy of formation of the IP-dimer ($\Delta E_{B\text{-ion-pair}}$)cluster with twice the binding energy of the front IP structure (-395.01 kJ/mol) gives a energy approximately equal to the IP-dimer binding energy from the constituent ions.

The dispersion energy contribution for the IP-dimer is found to be ≈50 kJ/mol and ≈45kJ/mol for the low-energy middle and diagonal structures. This energy is made up of the dispersion energy of the formation of two IPs ≈14 kJ/mol (7+7, Table S1) and the energy on the formation of the IP-dimer ≈25-35kJ/mol, calculated as the difference of the B3LYP-D3 and B3LYP $\Delta E_B'$ energies in Table S9.

H. Energy bands

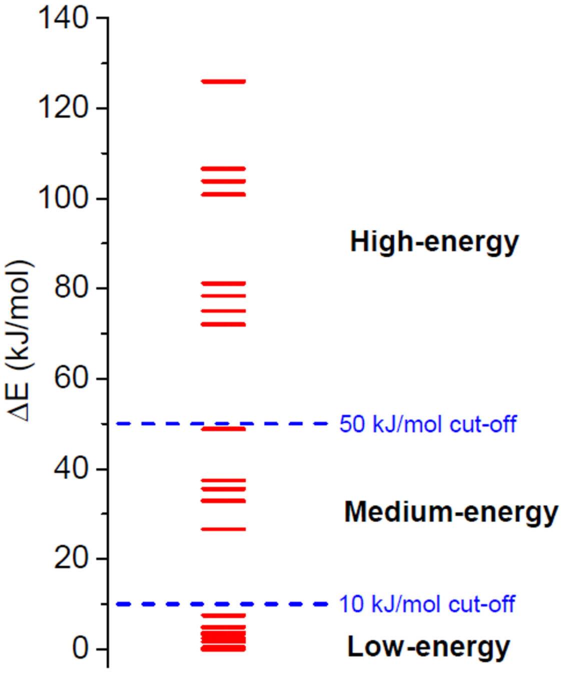

Figure S5. Plot of ΔE (kJ/mol) of the [C1C1im]Cl IP-dimers at the B3LYP-D3 level.

I. Data for [C$_1$C$_1$im]Cl IP-dimers

Table S10. Free energy (ΔG), Enthalpy (ΔH) and Entropy (TΔS), in kJ/mol, for the [C$_1$C$_1$im]Cl IP dimer M_FS_SF_A conformer.

	ΔG	**ΔH**	**TΔS**
B3LYP	-753.82	-858.39	-104.57
ωB97X	-798.09	-911.25	-113.16
MP2	-838.91	-907.84	-117.08
B3LYP-D2	-796.52	-912.89	-116.38
ωB97X-D	-790.76	-907.84	-117.08
B3LYP-D3	-799.60	-912.59	-113.00

Table S11. Relative conformer free energies (ΔΔG), in kJ/mol, for the [C$_1$C$_1$im]Cl IP dimers in the low- and medium-energy bands reported relative to the M_FS_SF_A conformer.

	B3LYP	**ωB97X**	**MP2**	**B3LYP-D2**	**ωB97X-D**	**B3LYP-D3**
M_FS_SF_A	0.00	0.00	0.00	0.00	0.00	0.00
M_FS_SF_R	Not Stable	0.21	-5.90	0.53	0.13	0.23
M_FS_FS_R	0.26	0.97	0.31	2.27	0.01	0.60
D_F1T_TF_A	-3.89	-10.63	2.00	-0.33	-5.04	-2.33
D_F2T_TF_A	-1.23	-8.33	2.66	-0.21	-4.98	-2.10
D_F1T_TF_T	-2.38	-8.29	4.50	0.11	-2.58	-1.75
D_F2T_TF_T	0.13	-6.46	6.43	1.42	-0.11	0.56
M_FS_SF_P	5.59	Not Stable	4.07	7.82	6.14	5.85
M_SS_SS_A	17.62	19.20	23.70	19.13	23.57	20.99
D_TM_BF_T	15.03	19.99	36.87	25.60	23.79	34.97
D_TB_BT_A	Not Stable	26.69	25.75	31.20	29.52	29.70
M_FB_BF_A	Not Stable	Not Stable	26.86	31.61	31.40	30.76
D_TBt_BB_P	Not Stable	35.60	33.58	38.14	Not Stable	36.59

Table S12. Relative enthalpies (ΔΔH), in kJ/mol, for the [C$_1$C$_1$im]Cl IP dimers in the low- and medium-energy bands reported relative to the M_FS_SF_A conformer.

	B3LYP	**ωB97X**	**MP2**	**B3LYP-D2**	**ωB97X-D**	**B3LYP-D3**
M_FS_SF_A	0.00	0.00	0.00	0.00	0.00	0.00
M_FS_SF_R	Not Stable	1.36	-5.97	2.07	-0.21	0.35
M_FS_FS_R	0.80	1.34	1.33	3.05	2.20	1.89
D_F1T_TF_A	-2.14	-3.52	12.38	8.15	6.00	3.53
D_F2T_TF_A	-0.08	-1.88	11.90	9.60	6.83	4.57
D_F1T_TF_T	-0.68	-1.74	13.94	10.01	7.89	5.14
D_F2T_TF_T	1.71	-0.18	15.74	10.79	9.20	6.21
M_FS_SF_P	5.49	Not Stable	2.80	9.43	7.73	7.71
M_SS_SS_A	15.84	24.07	36.39	31.03	31.37	28.08
D_TM_BF_T	23.94	30.00	51.39	38.93	38.57	34.97
D_TB_BT_A	Not Stable	37.24	42.97	42.48	43.39	37.55
M_FB_BF_A	Not Stable	Not Stable	34.23	39.65	40.23	39.17
D_TBt_BB_P	Not Stable	49.33	54.06	56.61	Not Stable	51.84

Table S13. Relative entropies (ΔTΔS) in kJ/mol for the [C_1C_1im]Cl IP dimers in the low- and medium-energy bands reported relative to the M_FS_SF_A conformer.

	B3LYP	***ω*B97X**	**MP2**	**B3LYP-D2**	***ω*B97X-D**	**B3LYP-D3**
M_FS_SF_A	0.00	0.00	0.00	0.00	0.00	0.00
M_FS_SF_R	Not Stable	1.16	-0.07	1.54	-0.33	0.13
M_FS_FS_R	0.54	0.38	1.02	0.77	2.19	1.29
D_F1T_TF_A	1.75	7.11	10.38	8.48	11.04	5.85
D_F2T_TF_A	1.16	6.44	9.24	9.81	11.81	6.67
D_F1T_TF_T	1.70	6.54	9.44	9.90	10.47	6.89
D_F2T_TF_T	1.58	6.29	9.31	9.36	9.31	5.65
M_FS_SF_P	-0.10	Not Stable	-1.27	1.61	1.59	1.86
M_SS_SS_A	-1.78	4.87	12.69	11.90	7.80	7.10
D_TM_BF_T	8.91	10.01	14.52	13.33	14.77	9.97
D_TB_BT_A	Not Stable	10.55	17.23	11.27	13.87	7.86
M_FB_BF_A	Not Stable	Not Stable	7.37	8.04	8.83	8.41
D_TBt_BB_P	Not Stable	13.73	20.48	18.47	Not Stable	15.26

Table S14. ZPE and BSSE corrections, in kJ/mol, for the [C_1C_1im]Cl IP-dimer M_FS_SF_A conformer calculated at various levels of theory.

	ZPE (kJ/mol)	**BSSE (kJ/mol)**
B3LYP	739.93	1.61
***ω*B97X**	752.18	2.21
MP2	745.73	66.06
B3LYP-D2	738.94	2.26
***ω*B97X-D**	749.97	2.14
B3LYP-D3	741.35	2.12

Table S15. Relative zero-point energy corrections (ΔZPE) in kJ/mol for the [C_1C_1im]Cl IP-dimers in the low- and medium-energy bands calculated at various levels of theory reported relative to the M_FS_SF_A conformer.

	B3LYP	***ω*B97X**	**MP2**	**B3LYP-D2**	***ω*B97X-D**	**B3LYP-D3**
M_FS_SF_A	0.00	0.00	0.00	0.00	0.00	0.00
M_FS_SF_R	Not Stable	-0.72	-0.79	-0.90	-0.75	-0.58
M_FS_FS_R	-0.06	0.08	-0.37	-0.30	-0.08	-0.34
D_F1T_TF_A	0.08	-0.75	-0.12	-0.31	-1.27	0.06
D_F2T_TF_A	0.35	-0.42	-0.27	-0.36	-1.42	0.08
D_F1T_TF_T	0.12	-0.52	0.28	-0.48	-1.13	0.00
D_F2T_TF_T	0.31	-0.43	0.40	-0.43	-0.56	0.22
M_FS_SF_P	0.34	Not Stable	0.37	-0.17	-0.66	0.09
M_SS_SS_A	0.12	-0.40	-1.04	-2.35	-1.04	-1.09
D_TM_BF_T	-1.91	-2.12	-2.11	-2.27	-3.26	-1.71
D_TB_BT_A	Not Stable	-1.54	-2.81	-1.01	-2.03	-0.45
M_FB_BF_A	Not Stable	Not Stable	-2.36	-2.20	-1.58	-1.93
D_TBt_BB_P	Not Stable	-2.36	-3.63	-2.06	Not Stable	-1.57

Table S16. Relative BSSE (ΔBSSE) in kJ/mol for the [C_1C_1im]Cl IP dimers in the low- and medium-energy bands calculated at various levels of theory reported relative to the M_FS_SF_A conformer.

	B3LYP	**ωB97X**	**MP2**	**B3LYP-D2**	**ωB97X-D**	**B3LYP-D3**
M_FS_SF_A	0.00	0.00	0.00	0.00	0.00	0.00
M_FS_SF_R	Not Stable	0.03	5.66	0.12	0.14	0.10
M_FS_FS_R	0.00	-0.09	-2.10	-0.07	-0.07	-0.09
D_F1T_TF_A	-0.04	-0.50	-10.96	-0.52	-0.52	-0.40
D_F2T_TF_A	-0.01	-0.49	-9.04	-0.53	-0.51	-0.40
D_F1T_TF_T	-0.11	-0.55	-10.15	-0.60	-0.57	-0.46
D_F2T_TF_T	-0.07	-0.55	-10.86	-0.59	-0.58	-0.46
M_FS_SF_P	0.00	Not Stable	4.25	0.03	0.04	-0.01
M_SS_SS_A	-0.14	-0.72	-15.72	-0.70	-0.68	-0.59
D_TM_BF_T	-0.16	-0.65	-17.11	1.16	0.21	-0.49
D_TB_BT_A	Not Stable	-0.45	-10.73	-0.43	-0.40	-0.32
M_FB_BF_A	Not Stable	Not Stable	0.94	0.01	0.00	-0.06
D_TBt_BB_P	Not Stable	-0.48	-12.11	-0.48	Not Stable	-0.37

J. RDF of COR-COR for [C_2C_1im]Cl

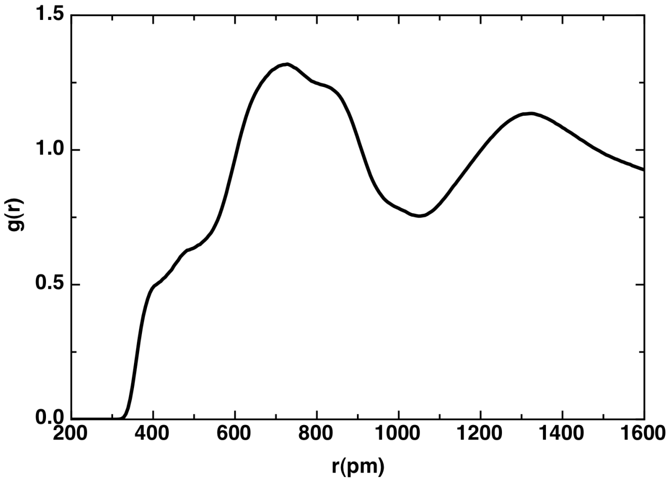

Figure S6. RDF of centre of ring (COR) to COR for [C_2C_1im]Cl. The pre-peak at 400-500pm indicates the region for π-stacking interactions.

K. π^+-π^+ stacked structures from MD trajectories

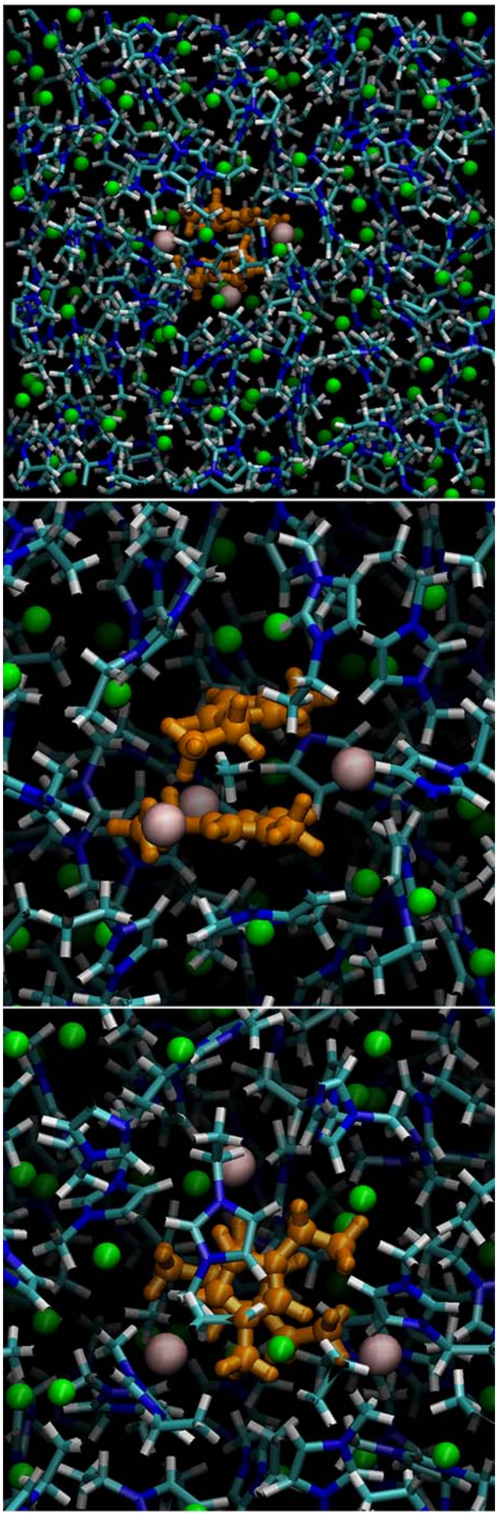

Figure S7: Top and side views of cation stacking and chloride anions on the periphery obtained from MD trajectories.

L. Scan of the Potential energy surface joining M_FS_SF_R and D_F1T_TF_A

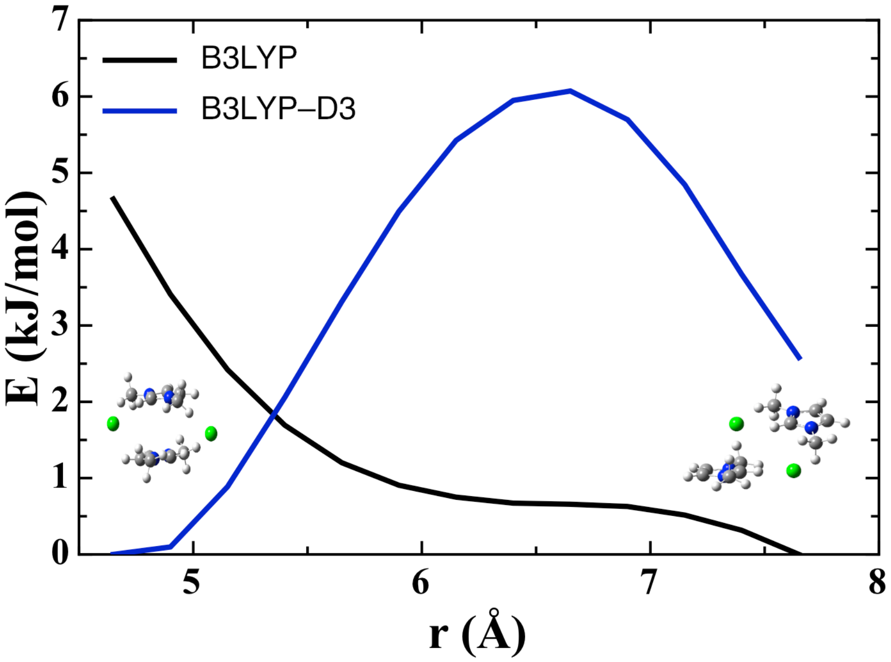

Figure S8: Relative potential energy profiles (kJ/mol) for the relaxed scan of the distance (Å) between C^4 carbons computed at the B3LYP (dashed line) and B3LYP-D3 (solid line) levels.

Potential energy profiles have been computed using a relaxed scan (0.25 Å steps; starting at ≈4.65 Å) connecting the C^4 atoms of each $[C_1C_1im]^+$ ring at the B3LYP/aug-cc-pVTZ (black) and B3LYP-D3/aug-cc-pVTZ (blue) levels.